

$X(3960)$ seen in $D_s^+ D_s^-$ as the $X(3930)$ state seen in $D^+ D^-$

M. Bayar,^{1,2,*} A. Feijoo^{2,†} and E. Oset^{2,‡}

¹*Department of Physics, Kocaeli University, Izmit 41380, Turkey*

²*Departamento de Física Teórica and IFIC, Centro Mixto Universidad de Valencia-CSIC Institutos de Investigación de Paterna, Apartado 22085, 46071 Valencia, Spain*

 (Received 21 July 2022; accepted 13 January 2023; published 8 February 2023)

We perform a calculation of the interaction of the $D\bar{D}$, $D_s\bar{D}_s$ coupled channels and find two bound states, one coupling to $D\bar{D}$ and another one at higher energies coupling mostly to $D_s^+ D_s^-$. We identify this latter state with the $X_0(3930)$ seen in the $D^+ D^-$ mass distribution in the $B^+ \rightarrow D^+ D^- K^+$ decay, and also show that it produces an enhancement of the $D_s^+ D_s^-$ mass distribution close to threshold which is compatible with the recent LHCb observation in the $B^+ \rightarrow D_s^+ D_s^- K^+$ decay which has been identified as a new state, $X_0(3960)$.

DOI: [10.1103/PhysRevD.107.034007](https://doi.org/10.1103/PhysRevD.107.034007)

I. INTRODUCTION

In a recent talk at CERN [1], and subsequent preprint [2], the LHCb Collaboration reported on three new states one of which, named as $X(3960)$, is seen as a peak in the $D_s^+ D_s^-$ mass distribution of the $B^+ \rightarrow D_s^+ D_s^- K^+$ decay. The properties assigned to that state are

$$J^{PC} = 0^{++}; \quad M_0 = 3955 \pm 6 \pm 11 \text{ MeV},$$

$$\Gamma_0 = 48 \pm 17 \pm 10 \text{ MeV}.$$

The peak is remarkably close to the $D_s^+ D_s^-$ threshold, 3937 MeV, which makes one wonder whether it could not be a signal for a resonance just below threshold.¹ This is actually a well-known feature of reactions as discussed in [3] and found in some specific reactions [4,5]. Actually, the B^+ decay into $B^+ \rightarrow D^+ D^- K^+$ showed a signal in the $D^- D^+$ mass distribution for a 0^{++} state, branded $X_0(3930)$, with properties [6,7]

$$J^{PC} = 0^{++}; \quad M'_0 = 3924 \pm 2 \text{ MeV}, \quad \Gamma'_0 = 17 \pm 5 \text{ MeV}.$$

If the $X_0(3930)$ state is coupled both to $D^+ D^-$ and $D_s^+ D_s^-$, that state would necessarily produce an enhancement close to threshold in the $D_s^+ D_s^-$ mass distribution,

which could explain the experimental observation without the need to introduce an extra resonance. The purpose of this work is to show that present dynamics of the interaction of charmed mesons leads naturally to this conclusion.

The first consideration in this respect is the QCD lattice result of [8], where a 0^{++} bound state coupling strongly to $D_s^+ D_s^-$ and weakly to $D^+ D^-$ is found below the $D_s^+ D_s^-$ threshold. Such a state would indeed show a peak in the $D^+ D^-$ mass distribution and an enhanced mass distribution of the $D_s^+ D_s^-$ around threshold.

One might expect that such a state would appear in a dynamical study of $D\bar{D}$ and $D_s^+ D_s^-$ in coupled channels. Interestingly, this study has been done in [9–11], where a $D\bar{D}$ bound state was found, yet no bound state was found close to the $D_s^+ D_s^-$ threshold coupling mostly to that channel.

In what follows we show that this is a consequence of the strong $D\bar{D} \rightarrow D_s^+ D_s^-$ transition, to the point that a little weaker transition, which finds a natural explanation here, already gives rise to the two states; the upper one coupled mostly to $D_s^+ D_s^-$ as in [8] and with properties that are consistent with the mass and width of the $X_0(3930)$, and the strength and shape of the $D_s^+ D_s^-$ mass distribution of the $X_0(3960)$. A formulation of the problem is presented below.

II. FORMALISM

We depart from the dynamics of the $D\bar{D}$, and coupled channels used in [9] and use a formulation based on the extension of the local hidden-gauge approach [12–15], which has turned out to make accurate predictions for $D^{(*)} K^{(*)}$ and $D^{(*)} \bar{K}^{(*)}$ states [16,17] or T_{cc} and related states [18,19] among others. The dynamics are based on the exchange of vector mesons as depicted in Fig. 1.

One needs the VPP ($V = \text{vector}$, $P = \text{pseudoscalar}$) vertex given by

*melahat.bayar@kocaeli.edu.tr

†edfeijoo@ific.uv.es

‡oset@ific.uv.es

¹Comment of Sasa Prelovsek in the discussion of the talk [1].

$$\begin{aligned}\mathcal{L}_{VPP} &= -ig\langle [P, \partial_\nu P]V^\nu \rangle, \\ g &= \frac{M_V}{2f} (M_V \simeq 800 \text{ MeV}, f = 93 \text{ MeV}),\end{aligned}\quad (1)$$

where P and V are the $q_i\bar{q}_j$ matrices written in terms of pseudoscalar (P) and vector (V) mesons, respectively

$$P = \begin{pmatrix} \frac{1}{\sqrt{2}}\pi^0 + \frac{1}{\sqrt{3}}\eta + \frac{1}{\sqrt{6}}\eta' & \pi^+ & K^+ & \bar{D}^0 \\ \pi^- & -\frac{1}{\sqrt{2}}\pi^0 + \frac{1}{\sqrt{3}}\eta + \frac{1}{\sqrt{6}}\eta' & K^0 & D^- \\ K^- & \bar{K}^0 & -\frac{1}{\sqrt{3}}\eta + \sqrt{\frac{2}{3}}\eta' & D_s^- \\ D^0 & D^+ & D_s^+ & \eta_c \end{pmatrix}, \quad (2)$$

$$V = \begin{pmatrix} \frac{1}{\sqrt{2}}\rho^0 + \frac{1}{\sqrt{2}}\omega & \rho^+ & K^{*+} & \bar{D}^{*0} \\ \rho^- & -\frac{1}{\sqrt{2}}\rho^0 + \frac{1}{\sqrt{2}}\omega & K^{*0} & \bar{D}^{*-} \\ K^{*-} & \bar{K}^{*0} & \phi & D_s^{*-} \\ D^{*0} & D^{*+} & D_s^{*+} & J/\psi \end{pmatrix}, \quad (3)$$

and $\langle \rangle$ means the trace of the $q_i\bar{q}_j$ matrices. Although formally one is using an $SU(4)$ formalism, in this particular case with the use of Eq. (1) one is only making use of the $q\bar{q}$ nature of the different mesons, as shown in Sec. II A of [20].

A straightforward calculation of the diagrams of Fig. 1 with the Lagrangian of Eq. (1) considering the channels $D\bar{D}$, $I = 0$, and $D_s^+D_s^-$ with the $(D^+, -D^0)(\bar{D}^0, D^-)$ multiplets

$$(D\bar{D}, I = 0) = \frac{1}{\sqrt{2}}(D^+D^- + D^0\bar{D}^0); D_s^+D_s^-,$$

and neglecting q^2 in the $(q^2 - M_V^2)^{-1}$ propagators gives the interaction potential

$$V_{ij} = -B_{ij}g^2(p_1 + p_3)(p_2 + p_4), \quad (4)$$

with

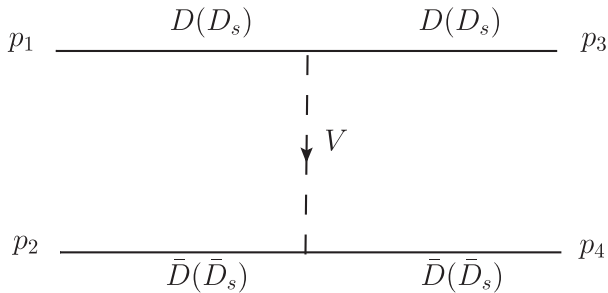


FIG. 1. Dynamics of $D(D_s) \rightarrow \bar{D}(\bar{D}_s)$ interaction due to vector exchange.

$$B = \begin{pmatrix} \frac{1}{2}\left(\frac{3}{M_\rho^2} + \frac{1}{M_\omega^2} + \frac{2}{M_{J/\psi}^2}\right) & \sqrt{2}\frac{1}{M_{K^*}^2} \\ \sqrt{2}\frac{1}{M_{K^*}^2} & \left(\frac{1}{M_\phi^2} + \frac{1}{M_{J/\psi}^2}\right) \end{pmatrix}, \quad (5)$$

and projected over the S -wave we have

$$\begin{aligned}(p_1 + p_3)(p_2 + p_4) &\rightarrow \frac{1}{2}\left[3s - (m_1^2 + m_2^2 + m_3^2 + m_4^2)\right. \\ &\quad \left. - \frac{1}{s}(m_1^2 - m_2^2)(m_3^2 - m_4^2)\right].\end{aligned}\quad (6)$$

The unitarization via the Bethe-Salpeter (BS) equation gives the scattering matrix

$$T = [1 - VG]^{-1}V, \quad (7)$$

where G is the loop function for two meson intermediate states that we choose to regularize with dimensional regularization as we did in [9].

The G function that we use has both real and imaginary parts, which makes the approach different to a K matrix approach which is equivalent to the present one keeping only ImG . While this latter approach respects fully unitarity, it misses the nonregular structure of ReG , with a cusp around threshold, which makes our approach better suited to study amplitudes around thresholds as in the present case.

The exchange of the vector mesons for the interaction of mesons is based on the local hidden gauge approach [12–15] extrapolated to the charm sector. In the $SU(3)$ sector the equivalence of the local hidden gauge approach and chiral

Lagrangians was established in [21]. An explicit easy derivation for the case of vector-pseudoscalar interaction is given in Appendix A of Ref. [22]. While the derivation of chiral Lagrangians results from the consideration of symmetries of QCD, among them chiral symmetry, suited to the case of light quarks, the englobing local hidden-gauge approach is not restricted by light quark masses and can be extrapolated to the heavy quark sector, as we do here and has been done in many other works (see recent reviews [23,24]).

Equation (7) results from the on shell factorization of the potential in the Bethe-Salpeter equation $T = V + VGT$ with relativistic propagators and integration over four momenta in the loops. There are many ways to justify this on shell factorization. In [25,26] it was shown that off shell effects within the BS equation can be reabsorbed into the on shell potential through a proper renormalization. A different derivation of the same results can be obtained using a separable potential as shown in [27]. Finally, a useful derivation can be done using dispersion relations for T^{-1} , which provide the full analytical structure of the amplitude, and neglecting the left-hand cut in the dispersion relation [28]. The left-hand cut produces a small contribution [29], but more importantly, it is very weakly energy dependent in the physical region of interest in scattering. Hence, it can be reabsorbed easily in the G function, which contains a subtraction constant in dimensional regularization, or a q_{\max} cutoff regularization, which finally are fine-tuned to data to obtain for instance the precise mass of a given state.

An interesting thing happens with Eq. (7). If we eliminate the V_{12} term of Eq. (4) which connects the $D^+ D^-$ and $D_s^+ D_s^-$ channels, we get two poles with ordinary values of the subtraction constant $a \sim -1.5$ of the G function in a wide range of values, meaning that the two V_{11}, V_{22} potentials are strong enough to bind the $D\bar{D}$ and $D_s\bar{D}_s$ components. Yet, when V_{12} is switched on, the $D\bar{D}$ state remains and the $D_s\bar{D}_s$ state disappears. This is what happened in [9] where the $D_s\bar{D}_s$ state was not found. Curiously, if we weaken V_{12} to a value of about 70% of its strength in Eq. (5) the two states already appear.

Actually, it is easy to see that a more accurate calculation keeping q^2 in the vector meson propagator produces that reduction of V_{12} . In the diagonal terms of the matrix of Eq. (5), for instance $D\bar{D} \rightarrow D\bar{D}$ transition evaluated close to threshold, we have $q^0 = 0$ and $\vec{q} \sim 0$. Then the exchanged vector propagator becomes $(1/-M_V^2)$ as we have assumed. However, for the $D\bar{D} \rightarrow D_s\bar{D}_s$ transition calculated at the $D_s\bar{D}_s$ threshold we have

$$q^2 = (p_D - p_{D_s})^2 = p_D^2 + p_{D_s}^2 - 2p_D p_{D_s} = M_D^2 - M_{D_s}^2.$$

Hence in Eq. (5) we must replace in the nondiagonal terms

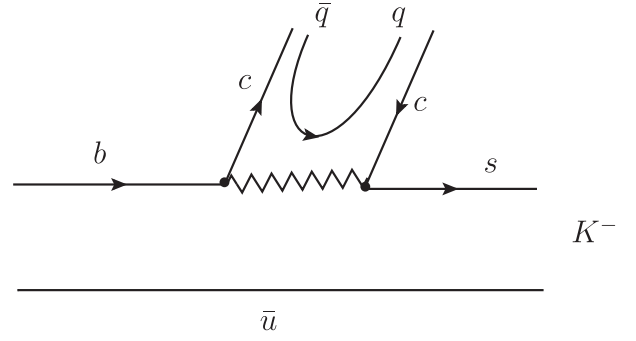


FIG. 2. B^- decay via internal emission at the quark level and hadronization.

$$\frac{1}{M_{K^*}^2} \rightarrow \frac{1}{M_{K^*}^2 + M_{D_s}^2 - M_D^2} \quad (8)$$

and the ratio of the new term to the former one is 0.68, which already gives rise to the appearance of the basically $D_s\bar{D}_s$ state.

The next, nontrivial, step is to relate the $D^+ D^-$ and $D_s^+ D_s^-$ mass distributions. We use the charge conjugate reactions $B^- \rightarrow D^+ D^- K^-$, $D_s^+ D_s^- K^-$ and have

$$\frac{d\Gamma}{dM_{\text{inv}}} = \frac{1}{(2\pi)^3} \frac{1}{4M_B^2} p_{K^-} \tilde{p}_{D_i} |\tilde{t}_i|^2, \quad (9)$$

where p_{K^-} is the K^- momentum in the B^- rest frame, and \tilde{p}_{D_i} the D^+ or D_s^+ momenta in the $D^+ D^-$, $D_s^+ D_s^-$ rest frame, respectively. The matrices \tilde{t}_i stand for the transitions $B^- \rightarrow D^+ D^- K^-$ and $D_s^+ D_s^- K^-$ and are constructed in the following way. The B^- decays proceed via interval emission [30], as depicted in Fig. 2, and are related.

The $c\bar{c}$ pair is hadronized and we have

$$\begin{aligned} c\bar{c} &\rightarrow \sum_i c\bar{q}_i q_i \bar{c} \rightarrow \sum_i P_{4i} P_{i4} = D^0 \bar{D}^0 + D^+ D^- + D_s^+ D_s^- \\ &= \sqrt{2} D\bar{D} + D_s^+ D_s^-, \end{aligned} \quad (10)$$

where we have eliminated $\eta_c \eta_c$ which plays no role here. Once $D\bar{D}$ and $D_s^+ D_s^-$ have been created, they propagate as shown in Fig. 3.

Then we immediately obtain

$$\begin{aligned} \tilde{t}_{D^+ D^-} &= C(1 + G_{D\bar{D}}(M_{\text{inv}}) T_{D\bar{D}, D\bar{D}}(M_{\text{inv}}) \\ &+ \frac{1}{\sqrt{2}} G_{D_s\bar{D}_s}(M_{\text{inv}}) T_{D_s\bar{D}_s, D\bar{D}}(M_{\text{inv}})), \end{aligned} \quad (11)$$

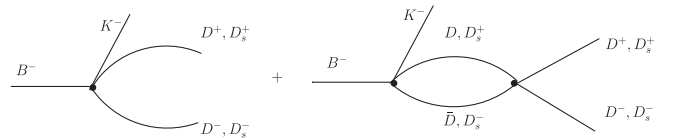


FIG. 3. Production and propagation of the $D^+ D^-$ and $D_s^+ D_s^-$ components through final-state interaction.

TABLE I. Masses and widths of the poles dynamically generated by the model, as well as, the corresponding modulus of the couplings $|g_i|$.

| | M [MeV] | Γ [MeV] | $ g_{D\bar{D}} $ [MeV] | $ g_{D_s\bar{D}_s} $ [MeV] |
|-------------------------|--------------|-------------------|---------------------------|-------------------------------|
| Pole I | 3699.04 | ... | 14509.0 | 5707.2 |
| Pole II ($X_0(3930)$) | 3932.72 | 12.32 | 2889.5 | 10018.0 |

$$\begin{aligned} \tilde{t}_{D_s^+ D_s^-} = & C(1 + \sqrt{2}G_{D\bar{D}}(M_{\text{inv}})T_{D\bar{D},D_s^+ D_s^-}(M_{\text{inv}})) \\ & + G_{D_s\bar{D}_s}(M_{\text{inv}})T_{D_s^+ D_s^-,D_s^+ D_s^-}(M_{\text{inv}}), \end{aligned} \quad (12)$$

with C an arbitrary constant. We can see that the D^+D^- and $D_s^+D_s^-$ production rates are related via the dynamics of the process and we can also test the relative strength of the two distributions.

III. RESULTS

We then proceed as follows. We choose a value of the subtraction constant $a_{D_s\bar{D}_s}$ of $G_{D_s\bar{D}_s}$ such as to get approximately the right mass of the $X_0(3930)$ state. We accomplish this with the value

$$a_{D_s\bar{D}_s} = -1.58 \quad (13)$$

within the natural range suggested in [28]. At the same time we choose $a_{D\bar{D}} = -1$ to get a $D\bar{D}$ bound state around 3700 MeV, as in [9],² and, considering the replacement of Eq. (8), we get the results in Table I. These results indicate that the lower state (*I*) couples more strongly to $D\bar{D}$ while the second state (*II*) couples more strongly to $D_s\bar{D}_s$ as found in [8].

In Fig. 4, we show the results for $\frac{d\Gamma}{dM_{\text{inv}}(D^+D^-)}$ and $\frac{d\Gamma}{dM_{\text{inv}}(D_s^+D_s^-)}$. The constant C has been chosen such as to have the normalization of the data for $\frac{d\Gamma}{dM_{\text{inv}}(D_s^+D_s^-)}$. We do not add a background to the distributions as in [1], since our amplitude \tilde{t}_i of Eqs. (11) and (12) already contain background through the terms 1 in the parenthesis (tree level). We observe that, with the chosen parameter of Eq. (13) that leads approximately to the properties of the $X_0(3930)$ state, we obtain a shape for $\frac{d\Gamma}{dM_{\text{inv}}(D_s^+D_s^-)}$ compatible with the experiment. It is also welcome the fact that the integrated strengths of the mass distributions for the D^+D^- and $D_s^+D_s^-$ peaks gives a ratio of $D_s^+D_s^-$ to D^+D^- of the order of 3, in agreement with experiment [2].

²Values of $a_{D\bar{D}}$ of the order of -1.3 were used in [9] to get that binding, but also many other light channels were considered (see also [31]) and it is well-known that there is a certain trade off between terms in the potential and changes in the G function.

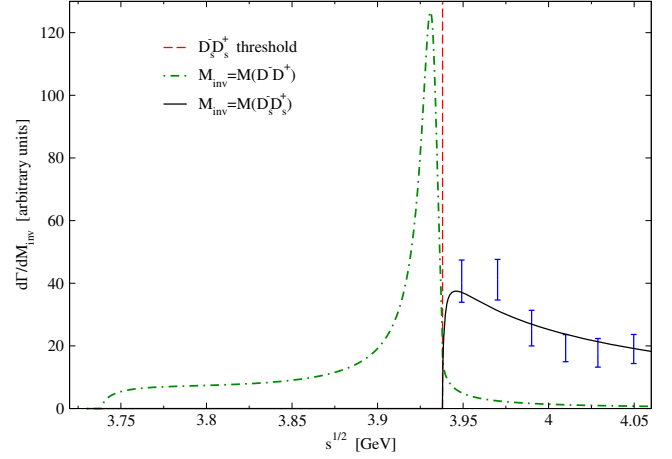


FIG. 4. $\frac{d\Gamma}{dM_{\text{inv}}(D^+D^-)}$ and $\frac{d\Gamma}{dM_{\text{inv}}(D_s^+D_s^-)}$ of $B^- \rightarrow D^+D^-K^-$ and $B^- \rightarrow D_s^+D_s^-K^-$ decays. The experimental points are taken from [1].

IV. CONCLUSIONS

In summary, we have shown that a state below the $D_s\bar{D}_s$ threshold, coupling strongly to $D_s\bar{D}_s$ and more weakly to $D\bar{D}$, as found in the lattice QCD calculations, will necessarily produce a $D_s\bar{D}_s$ mass distribution with a strong enhancement close to the $D_s\bar{D}_s$ threshold. A quantitative evaluation of the D^+D^- and $D_s^+D_s^-$ mass distributions in the $B^- \rightarrow D^+D^-K^-$ and $B^- \rightarrow D_s^+D_s^-K^-$ decays, with small modifications in the input used to obtain many hadronic states, shows that a $D_s^+D_s^-$ bound state appears, which can be associated to the $X_0(3930)$, and this state, coupling both to $D\bar{D}$ and $D_s^+D_s^-$, produces an enhancement in the $D_s^+D_s^-$ mass distribution close to threshold with a shape and relative strength compared to D^+D^- production in agreement with experiment. The conclusion is then that there is not need to invoke a new $X_0(3960)$ state, and the experimental observation is due to the presence of the $X_0(3930)$.

ACKNOWLEDGMENTS

This work is partly supported by the Spanish Ministerio de Economía y Competitividad (MINECO) and European FEDER funds under Contract No. PID2020–112777 GB-I00, and by Generalitat Valenciana under Contract PROMETEO/2020/023. This project has received funding from the European Union Horizon 2020 research and innovation programme under the Program H2020-INFRAIA-2018-1, Grant Agreement No. 824093 of the STRONG-2020 project. The work of A.F. was partially supported by the Generalitat Valenciana and European Social Fund APOSTD-2021-112, and the Czech Science Foundation, GAČR Grant No. 19-19640S.

- [1] Chen Chen and Elisabetta Spadaro Norella, <https://indico.cern.ch/event/1176505/>.
- [2] LHCb Collaboration, [arXiv:2210.15153](https://arxiv.org/abs/2210.15153).
- [3] X. K. Dong, F. K. Guo, and B. S. Zou, *Few Body Syst.* **62**, 61 (2021).
- [4] A. Martinez Torres, K. P. Khemchandani, F. S. Navarra, M. Nielsen, and E. Oset, *Phys. Lett. B* **719**, 388 (2013).
- [5] E. Wang, H. S. Li, W. H. Liang, and E. Oset, *Phys. Rev. D* **103**, 054008 (2021).
- [6] R. Aaij *et al.* (LHCb Collaboration), *Phys. Rev. D* **102**, 112003 (2020).
- [7] R. Aaij *et al.* (LHCb Collaboration), *Phys. Rev. Lett.* **125**, 242001 (2020).
- [8] S. Prelovsek, S. Collins, D. Mohler, M. Padmanath, and S. Piemonte, *J. High Energy Phys.* **06** (2021) 035.
- [9] D. Gamermann, E. Oset, D. Strottman, and M. J. Vicente Vacas, *Phys. Rev. D* **76**, 074016 (2007).
- [10] J. Nieves and M. P. Valderrama, *Phys. Rev. D* **86**, 056004 (2012).
- [11] C. Hidalgo-Duque, J. Nieves, and M. P. Valderrama, *Phys. Rev. D* **87**, 076006 (2013).
- [12] M. Bando, T. Kugo, and K. Yamawaki, *Phys. Rep.* **164**, 217 (1988).
- [13] M. Harada and K. Yamawaki, *Phys. Rep.* **381**, 1 (2003).
- [14] U. G. Meissner, *Phys. Rep.* **161**, 213 (1988).
- [15] H. Nagahiro, L. Roca, A. Hosaka, and E. Oset, *Phys. Rev. D* **79**, 014015 (2009).
- [16] R. Molina, T. Branz, and E. Oset, *Phys. Rev. D* **82**, 014010 (2010).
- [17] R. Molina and E. Oset, *Phys. Lett. B* **811**, 135870 (2020).
- [18] A. Feijoo, W. H. Liang, and E. Oset, *Phys. Rev. D* **104**, 114015 (2021).
- [19] L. R. Dai, R. Molina, and E. Oset, *Phys. Rev. D* **105**, 016029 (2022).
- [20] S. Sakai, L. Roca, and E. Oset, *Phys. Rev. D* **96**, 054023 (2017).
- [21] G. Ecker, J. Gasser, H. Leutwyler, A. Pich, and E. de Rafael, *Phys. Lett. B* **223**, 425 (1989).
- [22] J. M. Dias, G. Toledo, L. Roca, and E. Oset, *Phys. Rev. D* **103**, 116019 (2021).
- [23] X. K. Dong, F. K. Guo, and B. S. Zou, *Commun. Theor. Phys.* **73**, 125201 (2021).
- [24] X. K. Dong, F. K. Guo, and B. S. Zou, *Prog. Phys.* **41**, 65 (2021).
- [25] J. A. Oller and E. Oset, *Nucl. Phys.* **A620**, 438 (1997); **A652**, 407(E) (1999).
- [26] E. Oset and A. Ramos, *Nucl. Phys.* **A635**, 99 (1998).
- [27] D. Gamermann, J. Nieves, E. Oset, and E. Ruiz Arriola, *Phys. Rev. D* **81**, 014029 (2010).
- [28] J. A. Oller and U. G. Meissner, *Phys. Lett. B* **500**, 263 (2001).
- [29] J. A. Oller and E. Oset, *Phys. Rev. D* **60**, 074023 (1999).
- [30] L. L. Chau, *Phys. Rep.* **95**, 1 (1983).
- [31] C. W. Xiao and E. Oset, *Eur. Phys. J. A* **49**, 52 (2013).